

# Inertia of stimulated Mandel'shtam-Brillouin scattering and nonthreshold reflection short pulses with reversal of the wave front

V. F. Efimkov, I. G. Zubarev, A. V. Kotov, A. B. Mironov, S. I. Mikhaïlov, G. A. Pasmanik, M. G. Smirnov, and A. A. Shilov

*P. N. Lebedev Physics Institute, USSR Academy of Sciences*  
(Submitted 17 January 1979)  
Zh. Eksp. Teor. Fiz. 77, 526-536 (August 1979)

Stimulated Mandel'shtam-Brillouin scattering of the weak component of radiation, with reversal of the wave front at below-threshold intensity in the field of a stronger pump component is investigated. A substantial contraction of the backscattered pulse is observed, when its duration is less than or comparable with the relaxation time of the hypersound; the reflection coefficient of the weak pump component becomes at the same time weaker than that of the strong component. These results are theoretically interpreted. A procedure for obtaining sufficiently short pulses with reversal of the wave front in a nonthreshold regime is proposed and simulated.

PACS numbers: 41.10.Hv

1. We have previously shown that in stationary stimulated Mandel'shtam-Brillouin scattering (SMBS) it is possible to realize nonthreshold reflection of a weak signal with reversal of its wave front (RWF) in the field of a strong wave for which the threshold of the stimulated scattering has been exceeded and the RWF conditions satisfied. It was also indicated that this scheme may turn out to be useful for RWF of pulses with duration  $\tau_p \sim 1$  nsec, which is comparable with the shortest lifetimes  $\tau_{ph}$  of acoustic phonons in a number of media such as, e.g.,  $CCl_4$ . Such pulses are needed for many applications and in particular for the production and investigation of laser plasma.

The difficulty of direct conversion of pulses having this duration in SMBS is due to the strong increase, in view of the nonstationary processes, of the threshold intensity of the exciting radiation, and the onset of various obstructing nonlinear phenomena such as optical breakdown, self-focusing, and others.

However, nonthreshold reflection takes place effectively only in the stationary case, when the characteristic time scales of the variation of the pulses are large enough compared with the hypersound relaxation time. In this case the reflection coefficients of the strong and weak pump components are equal. In SMBS of a short and, in the general case, broadband light pulse with a multimode transverse structure the principal role is assumed by nonstationary effects that lead to differences between the reflection coefficients, to a change in the form of the Stokes pulses compared with the corresponding pump pulses, and others. The present paper is devoted to a theoretical and experimental investigation of these phenomena.

2. It is well known that the RWF of spatially multimode radiation can be effected either in a light pipe or by ordinary focusing of the radiation with a lens into an active medium. In both cases the effect is due to the same cause and manifests itself similarly in a certain region of the parameters.<sup>2</sup> Nonthreshold reflections can also be obtained by both methods; in particular, in our earlier study<sup>1</sup> we obtained this scattering regime only in a light pipe, while in the present study we used

also focusing with a lens.

It is much simpler to calculate theoretically the reversal of the wave front of spatially multimode radiation in SMBS for a light pipe. However, the main features of the scattering process, which are connected with its nonstationary character, should be preserved also in the case of focusing of the radiation into the active medium with a lens. We shall therefore calculate below the regime of interest to us for the case of a light pipe.

Assume that the pump radiation consists of two orthogonal components

$$E_L = e_0(\eta) \mathcal{E}_0(\mathbf{r}_\perp, z) + e_1(\eta) \mathcal{E}_1(\mathbf{r}_\perp, z),$$

$$\int \mathcal{E}_0 \mathcal{E}_1^* d^2 r_\perp = \delta_{ij} \mathcal{P} \quad (i, j=0, 1).$$

Let us find how RWF of the weaker component  $e_1 (e_1 \ll e_0)$ , will occur in the Stokes component if the envelopes of both components are plane,  $|\mathbf{E}_{0,1}|^2 = I$ . We seek the solution of the system of truncated equations

$$\left( v \frac{\partial}{\partial \eta} + \frac{\partial}{\partial z} + \frac{i}{2k} \Delta_\perp \right) E_s = i g_1 P^* E_L, \quad (1)$$

$$\frac{\partial P}{\partial \eta} + \gamma P = i g_2 E_L E_s^*, \quad v = \frac{1}{v_s} + \frac{1}{v_L}, \quad (2)$$

that describe the SMBS at  $k_L = k_s = k$  in the form

$$E_s = c_0(z, \eta) \mathcal{E}_0^*(\mathbf{r}_\perp, z) + c_1(z, \eta) \mathcal{E}_1^*(\mathbf{r}_\perp, z) + \tilde{\mathcal{E}},$$

$$P = P_0(z, \eta) \mathcal{E}_0^2(\mathbf{r}_\perp, z) + P_1(z, \eta) \mathcal{E}_1^2(\mathbf{r}_\perp, z) + P_{01}(z, \eta) \mathcal{E}_0(\mathbf{r}_\perp, z) \mathcal{E}_1(\mathbf{r}_\perp, z) + \tilde{P}. \quad (3)$$

We assume that the components  $e_0 \mathcal{E}_0$  and  $e_1 \mathcal{E}_1$  correspond to multimode waves with divergence  $\sim \theta$ . Then the relative contributions of the components  $\tilde{\mathcal{E}}$  and  $\tilde{P}$  to the total power of the backscattered radiation is small if the total increment

$$M_k = g I |e_0|^2 / k_s \theta^2$$

( $g = g_1 g_2 / \gamma$ ) over the longitudinal correlation length  $z_k = 1/k_s \theta^2$  is small compared with unity<sup>2,3</sup>; in the nonstationary case

$$M_k = 2(2gI |e_0|^2 \gamma \eta (L-z))^{1/2}.$$

At  $M_k \ll 1$  the contribution of the components  $\bar{\mathcal{E}}$  and  $\bar{\mathcal{P}}$  is equivalent to the contribution from an additional delta-correlated source that excites the so-called "noise" waves (in the terminology of three-dimensional holography).<sup>3</sup> The noise contribution, however, can be comparable with the power of the weak component  $|c_1|^2 \mathcal{P}$ . In experiment, the weaker component  $e_1 \mathcal{E}_1$  with divergence  $\theta_1$  is passed through a phase plate that increases its divergence to a value  $\sim \theta \gg \theta_1$ . As a result of the RWF the Stokes component  $c_1$  that produces the field  $e_1$  passes through the same phase plate in the opposite direction and acquires thus again a divergence  $\theta_1$ . At the same time the noise in the Stokes radiation, with power  $\sim M_k |c_0|^2 \mathcal{P}$ , is uniformly distributed in an angle  $\sim \theta$  after passing through the phase plate. If the noise intensity in the solid angle  $\theta_1^2$  is small compared with the power  $|c_1|^2 \mathcal{P}$  of the Stokes wave that produces the field  $e_1 \mathcal{E}_1$ , i. e.,

$$\frac{\theta_1^2}{\theta^2} M_k |c_0|^2 \ll |c_1|^2, \quad (4)$$

then the contributions of the components  $\bar{\mathcal{E}}$  and  $\bar{\mathcal{P}}$  can be neglected. Thus, at  $\theta_1^2/\theta^2 \ll 1$  it is not essential to require that  $M_k$  be small compared with the ratio  $|c_1|^2/|c_0|^2$ , and it suffices only to have  $M_k \ll 1$ , and to satisfy the inequality (4). Then, substitution (3) in (1) and (2) and recognizing that  $\mathcal{E}_0$  and  $\mathcal{E}_1$  are orthogonal, we get after eliminating  $P_0$ ,  $P_1$ , and  $P_{01}$

$$\begin{aligned} v \frac{\partial c_0}{\partial \eta} + \frac{\partial c_0}{\partial z} = & -(g_1 g_2) \left\{ 2I e_0(\eta) \int_{-\infty}^{\eta} d\eta' e_0^*(\eta') c_0(z, \eta') \exp[-\gamma(\eta - \eta')] \right. \\ & \left. + I e_1(\eta) \int_{-\infty}^{\eta} d\eta' [e_0^*(\eta') c_1(z, \eta') + e_1^*(\eta') c_0(z, \eta')] \exp[-\gamma(\eta - \eta')] \right\}, \end{aligned} \quad (5)$$

$$\begin{aligned} v \frac{\partial c_1}{\partial \eta} + \frac{\partial c_1}{\partial z} = & -(g_1 g_2) \left\{ I e_0(\eta) \int_{-\infty}^{\eta} d\eta' [e_1^*(\eta') c_0(z, \eta') + e_0^*(\eta') c_1(z, \eta')] \right. \\ & \left. \times \exp[-\gamma(\eta - \eta')] + 2I e_1(\eta) \int_{-\infty}^{\eta} d\eta' e_1^*(\eta') c_1(z, \eta') \exp[-\gamma(\eta - \eta')] \right\}. \end{aligned} \quad (6)$$

The first term of the right-hand side of (5) and the last term of (6) describe the RWF of each of the pump waves when they propagate independently. The remaining two terms in the right-hand sides of each of these equations describe the coherent sources of the corresponding wave (due to the interaction of the three other waves) and the amplification of the wave in the mean field of the other pump component.

The stationary solution of the system (5) and (6) yields  $c_{0,1} = \text{const} \cdot e_{0,1}$ ; this corresponds to equality of the reflection coefficients of the strong and weak component, as was in fact observed by us experimentally in Ref. 1.

In the nonstationary case, however, the reflection coefficients can be different. Assume first that the stronger pump component has a constant average intensity  $|e_0(\eta)|^2 = \text{const}$ . We determine the values of  $c_0$  and  $c_1$ , neglecting the contribution of the component  $e_1 \mathcal{E}_1$  to the wave  $c_0 \mathcal{E}_0^*$ , as well as the contribution of this component  $e_1 \mathcal{E}_1$  to the amplification of its generating wave  $c_1 \mathcal{E}_1^*$ . We drop the last two terms in the right-hand side of (5) and the last term in the right-hand side of (6), a procedure justified when the intensi-

ty of the field  $e_1 \mathcal{E}_1$  is much lower than the threshold. Then neglecting the mismatch of the group velocities,  $\nu = 0$ , we find that the solution for  $c$  with the largest growth rate takes the form

$$\begin{aligned} c_0(z, \eta) = & a e_0(\eta) \exp[2gI |e_0|^2 (L-z)], \\ c_1(z, \eta) = & \frac{\gamma}{2} \frac{c_0(z, \eta)}{|e_0|^2} \int_{-\infty}^{\eta} d\eta' e_1^*(\eta') e_0(\eta') \exp\left(-\gamma \frac{\eta - \eta'}{2}\right). \end{aligned} \quad (7)$$

We assume that  $e_0(\eta) = 1$ , and that the weak component is a rectangular pulse in time

$$e_1(t) = \bar{e}_1 \begin{cases} 1, & 0 \leq t < t_0 \\ 0, & t \geq t_0 \end{cases} \quad (8)$$

We then obtain for the power of the reflected weak signal

$$|c_1(t)|^2 = |c_0|^2 |\bar{e}_1|^2 \begin{cases} (1 - e^{-\gamma t/2})^2, & 0 \leq t < t_0 \\ e^{-\gamma t} (e^{\gamma t_0/2} - 1)^2, & t \geq t_0 \end{cases} \quad (9)$$

The energy of the scattered weak component is

$$W_1 = \int_0^{\infty} dt |c_1(t)|^2 = |c_0|^2 |\bar{e}_1|^2 t_0 \left[ 1 - \frac{2}{\gamma t_0} (1 - e^{-\gamma t_0/2}) \right]. \quad (10)$$

Here  $|\bar{e}_1|^2 t_0$  is the energy of the incident weak wave, so that  $R_w = W_1/|\bar{e}_1|^2 t_0$  is its energy reflection coefficient. Since we have assumed the strong wave to be stationary and normalized to unity  $e_0(\eta) = 1$ , its power and energy reflection coefficients coincide and are equal to  $R_{str} = |c_0|^2$ . Thus, Eqs. (9) and (10) yield the connection between the corresponding reflection coefficients for the strong and weak waves:

$$\frac{R_w}{R_{str}} = 1 - \frac{2}{\gamma t_0} (1 - e^{-\gamma t_0/2}). \quad (11)$$

From the form of the solution (7), (9), it follows that the RWF of the weak component has a time delay. Furthermore, if the two pump components are independent, then at  $\nu = 0$  the power of the  $c_1 \mathcal{E}_1^*$  wave decreases with broadening of the frequency spectrum  $\Delta\omega$  of either of the two

$$|c_{1i}|^2 \sim \frac{\gamma}{\Delta\omega} |c_0|^2 |e_1|^2$$

or with increasing frequency mismatch between them. The inertia of the process is caused by the fact that after the end of the action of the pulse  $e_1 \mathcal{E}_1$  the stronger component  $e_0 \mathcal{E}_0$  still continues to be scattered by the hypersound grating produced by the Stokes wave  $c_0 \mathcal{E}_0^*$  excited by the strong component as well as by the weak pump component  $e_1 \mathcal{E}_1$ . From the fall-off time of the pulse of the Stokes component  $c_1 \mathcal{E}_1^*$  corresponding to the signal  $e_1 \mathcal{E}_1$  with the steep trailing edge it is possible to measure directly in experiment the hypersound relaxation time  $\tau_0 = 1/\gamma$ .

Assume now that the pulse  $e_0(\eta)$  is rectangular with amplitude  $\bar{e}_0$  and duration shorter than or of the order of the hypersound relaxation time. Then the nonstationary solution of Eq. (5) at  $\nu = 0$  takes the form<sup>4</sup>

$$\begin{aligned} c_0(z, \eta) = & a \frac{|e_0(\eta)|^2}{|\bar{e}_0(\eta)|^2} [\pi i (2gI |e_0|^2 \gamma \eta (L-z))]^{1/2} \\ & \times \exp\{-\gamma \eta + 2[2gI |e_0|^2 \gamma \eta (L-z)]^{1/2}\}, \end{aligned} \quad (12)$$

where

$$(2gI|e_0|^2\gamma\eta(L-z))^h \gg 1.$$

It follows from (12) that in contrast to stationary stimulated scattering in the present case the growth rate of the Stokes wave exceeds the growth rates of other waves not correlated with the pump by a factor  $\sqrt{2}$ . The value of  $c_1$  is obtained from the solution of Eq. (6) with the function  $c_0(z, \eta)$  specified by Eq. (12). As a result we obtain

$$c_1(z, \eta) = e_0(\eta)c_0(z, \eta)e_1^*(\eta)/2|e_0|^2. \quad (13)$$

To simplify the results, Eqs. (6) were solved with the Stokes wave specified on the boundary  $z=L$ . When account is taken of the noise source distributed in the medium, the preexponential factor in Eq. (12) for  $c_0$  changes, but the relation (13) between  $c_0$  and  $c_1$  remains in force. This is a consequence of the fact that the generating wave  $c_0\mathcal{E}_0^*$  is amplified in the field  $e_0\mathcal{E}_0$  with a larger growth rate than for the amplification of the wave  $c_1\mathcal{E}_1^*$  in the same field.

It is seen from (13) that the Stokes pulse  $c_1\mathcal{E}_1^*$  will be just as short as the pump pulse. The power reflection coefficient of the wave  $e_1\mathcal{E}_1$ , equal to  $R_1 = |c_1|^2/|e_1|^2$ , is negligibly small in the absence of the field  $e_0\mathcal{E}_0$  and is approximately equal to  $0.25R_0$  during the time of the pump pulse ( $R_0 = |c_0|^2/|e_0|^2$  is the reflection coefficient of the wave  $e_0\mathcal{E}_0$ ). The numerical coefficient  $1/2$  in (13) is due to the difference between the growth rates of the waves  $c_0\mathcal{E}_0^*$  and  $c_1\mathcal{E}_1^*$  when each of them is amplified in the pump field  $e_0\mathcal{E}_0$ .

3. A block diagram of the experimental setup is shown in Fig. 1. The driving generator was a neodymium laser with diffraction divergence and with pulse duration  $\sim 50$  nsec at half-height. Part of its radiation was diverted from one face by a thick glass plate (to prevent interference) to an amplifier and acted as the strong pump component. From the remainder of the beam we cut out by the standard technique (coaxial Pockels cell triggered by a light-spark discharge) a rectangular pulse of 10 nsec duration. This pulse was also diverted to the amplifier from the face of the glass plate and served as the weak pump component.

When focusing with a lens was used, the active media were liquid  $\text{CCl}_4$  and gaseous  $\text{SF}_6$  at a pressure  $p=20$  atm, while in the case of a light pipe media were liquid  $\text{CS}_2$  and methane ( $\text{CH}_4$ ) gas at pressure  $p=150$  atm. In the light-pipe experiments both waves were brought together on the phase plate, and the image of this illuminated region was projected with a lens of  $f=20$  cm onto the entry into the light pipe. The convergence angle of the beams on the phase plate was  $\sim 10^{-2}$  rad. A rectangular metallic light pipe of  $4 \times 4$  mm cross section and 90 cm length was placed in the cell with the methane, while for the  $\text{CS}_2$  we used a round glass light pipe of 3 cm diameter and 70 cm length. When the radiation was focused into the active medium by a lens ( $f=17$  cm), the beams ahead of the lens were parallel and intersected either in its focal plane or, using a glass wedge (shown dashed in Fig.

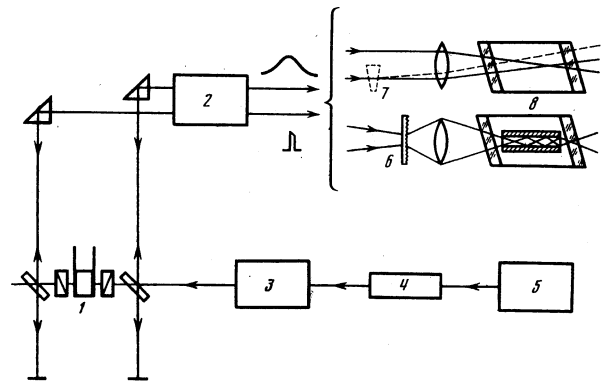


FIG. 1. Block diagram of experimental setup: 1—shutter, 2—amplifier, 3—preamplifier, 4—Faraday decoupler, 5—driving generator, 6—phase plate, 7—wedge, 8—cells.

1), the weak wave crossed the strong one ahead of the focal "neck".

We recorded in the experiment the distributions of the radiation in the backscattered waves (corresponding to the strong and weak components of the pump) in the near and far fields, their energies, as well as the pulse waveforms.

Figure 2 shows oscillograms of the pulse of the driving generator before and after we cut from it a rectangular pulse of 10 nsec duration. This pulse was cut from the leading front of the incident pulse for the following reasons. First, to compensate for the 10-nsec delay of the pulse in the system (see Fig. 1) and to synchronize its arrival at the Brillouin cell with the arrival of the maximum of the long pulse. Second, to make, if possible, the scattering in the direction of the weak wave, after the end of the short pulse, occur at a practically constant intensity of the strong wave.

To record the changes of the waveform of the backscattered Stokes wave, two pulses, incident and reflected, were applied to one sweep of the 12-7 oscilloscope. The first to be determined was the proper threshold of the reflection of the short pulse in the absence of the long one, and the waveform of the former was recorded. The intensity of the short pulse was then reduced with filters to below the threshold value and the signal of nonthreshold reflection of the weak wave was recorded in the presence of a strong wave of above-threshold intensity.

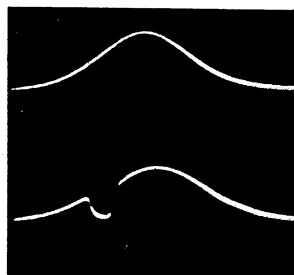


FIG. 2. Oscillograms of master-generator pulse before (upper) and after (lower) a rectangular pulse of 10 nsec duration is cut out of it.

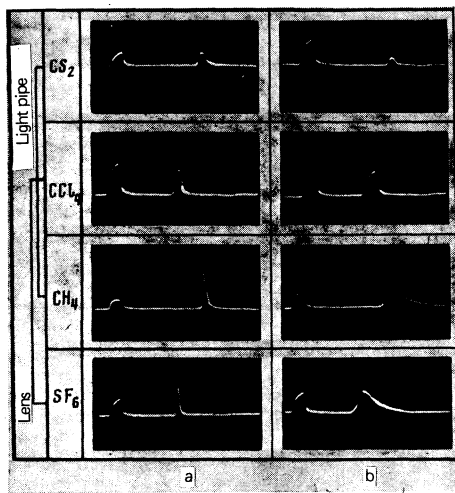


FIG. 3. Oscillograms of pulses of weak pump component (first pulse and of the component backscattered with reversal of its wave front (second pulse): a—intrinsic reflection, b—nonthreshold reflection.

The oscillograms of the corresponding pulses for the investigated media and for the methods used for their excitation are shown in Figs. 3 and 4. The first pulse on each oscillogram corresponds to the cut-out 10-nsec pulse incident on the cell. In the intrinsic reflection, the waveform of the backscattered Stokes pulse depends on the excess of the pump above threshold, and tends to have the shape of the pump if the excess is appreciable.

The shapes of the Stokes pulses in nonthreshold reflection in the field of the strong wave depend substantially on the quantity  $\gamma t_0 \approx 1$ . At  $\gamma t_0 \gg 1$  the backscattered Stokes wave duplicates in practice the weak pulse incident on the cell, and at  $\gamma t_0 \lesssim 1$  the leading and trailing edges of the reflected pulse are significantly drawn out. Figure 4 shows the waveforms of the reflected pulses, calculated from Eq. (9), for the cases  $\gamma t_0 \approx 1$ .

As already mentioned, knowing the attenuation of the trailing edge of the scattered pulse [see (9)] and for a steeply decreasing trailing edge, it is possible to measure directly the damping decrement of the hypersound  $\gamma = 1/\tau_{ph}$ . Reduction of the oscillograms of Fig. 3 yielded  $\tau_{ph} = 24 \pm 4$  nsec in  $CH_4$  and  $\tau_{ph} = 17 \pm 3$  nsec in  $SF_6$ . There are no published reports of measurement of these parameters at neodymium-laser frequency; the data obtained by us are in reasonable agreement with

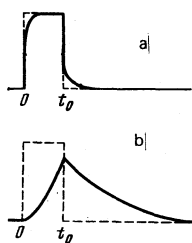


FIG. 4. Waveforms of reversed pulses in nonthreshold reflection of the weak rectangular pump component, calculated from Eq. (9) at  $\gamma t_0 \gg 1$  (a) and  $\gamma t_0 < 1$  (b).

their known analogs for ruby-laser frequencies.

The Stokes-pulse waveforms in nonthreshold reflection, shown in Fig. 4, were obtained assuming low intensity of the weak wave ( $e_1 \mathcal{E}_1 \ll e_0 \mathcal{E}_0$ ), when the amplification of the inverted Stokes radiation in the field of this wave and its influence on the reversal of the strong wave can be neglected. The coefficient of reflection of the weak pump component does not depend on the pump intensity [see (10)]. On the other hand when the intensity of the "weak" pump wave begins to approach the threshold of its intrinsic reflection, then the reflection coefficient and the waveform of the Stokes pulse, especially in the case when the radiation is focused with a lens, begin to depend on this intensity.

Figure 5 shows the reflection coefficients of the weak pump components (of 10 nsec duration) as functions of their intensity in  $CCl_4$  and  $SF_6$  when the radiation is focused with a lens. These functions were obtained at constant and identical reflection coefficients ( $R_{str} = 0.8$ ) of the strong pump components in the two media. The driving generator used in these experiments was not always single-frequency, and in many cases its emission had a fluctuating line width. This exerted no influence on the intrinsic reflection of the strong wave, owing to the short length of the focal "neck," 5 but the time delay of the weak component relative to the strong one led to a decrease of the reflection coefficient  $R_w$  of the weak component. The curves were therefore drawn only through averaged points with relatively large  $R_w$ .

In  $CCl_4$  the reflection of the weak component is practically stationary. The value of  $R_w$  is somewhat smaller than the strongwave reflection coefficient, apparently because of the small region of interaction of the spatially separated strong and weak pump components when they are focused into the cell by a lens (see Fig. 1) compared with the case of a light pipe.<sup>1</sup> Because of its large initial reflection coefficient in this case, it changes little when the rectangular-pulse intensity approaches the threshold value.

The nonthreshold reflection of the 10-nsec pulse in

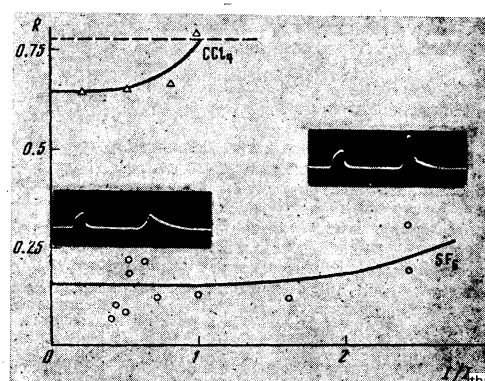


FIG. 5. Dependence of the reflection coefficients of the weak pump components on their intensities at constant reflection coefficients that are equal for both media (indicated by dashed line) of the strong components of the exciting radiation. The intensity is plotted in units of the stationary threshold values. The insets show oscillograms of the pulses for  $SF_6$  (similar to those of Fig. 3) at a much lower weak-component intensity, comparable with the threshold of the intrinsic reflection.

$SF_6$  is nonstationary. From Eq. (11) we get for  $SF_6$  at  $\gamma t_0 \approx 0.65$  the ratio  $R_w/R_{str} \approx 0.15$ . This value agrees well with experiment (Fig. 5) at low intensities (and in the region where the theory is valid). The nonstationary threshold of the intrinsic shortpulse reflection in  $SF_6$  exceeds the stationary threshold by 6–7 times. As the intensity of the cut-out pulse approaches the threshold value, its reflection coefficient tends to the stationary value. This changes also the waveform of the reflection coefficient, see the insets of Fig. 5; it is seen that amplification of the Stokes radiation comes into play during the action of the short pulse, whereas the exponentially damped tail remains unchanged.

It is well known<sup>2</sup> that a reversed Stokes component is produced in the region of the focal neck when the radiation is focused with a lens. Thus, when two parallel beams are focused by a lens they interact in the region of intersection of their focal necks, where the corresponding Stokes waves are formed (see Fig. 1). However, when the glass wedge shown dashed in Fig. 1 is introduced, the weak component crosses the strong-pump beam ahead of its focal neck, at a place where an already formed strong Stokes wave and a direct pump wave already exist. Nonthreshold reflection of the weak component is then also observed together with reversal of its wave front as well as all the singularities listed above.

This experiment can be regarded as reversal of the radiation wave front in a cell on which two opposing strong waves  $e_0\mathcal{E}_0$  and  $c_0\mathcal{E}_0^*$  are incident from the outside. Its peculiarity lies in the method of obtaining the strong wave  $c_0\mathcal{E}_0^*$  via the RWF effect, as a result of which these waves always have complex-conjugate fronts and, in principle, can have an arbitrary spatial structure.<sup>1)</sup>

We describe now the results on RWF of a weakquasi-continuous pump component in the field of another strong component of short pulse duration. This process was observed in experiment in the following manner (Fig. 1). The intensity of the cut-out pulse of 10 nsec duration was raised to a value above the threshold and this pulse served as the strong pump component; on the other hand the power of the quasicontinuous pulse diverted ahead of the cut-out system was attenuated with filters to a value considerably lower than the threshold, and this pulse acted as the weak pump component. The oscilloscope sweep recorded simultaneously the incident weakquasi-continuous pulse and the pulse with RWF reflected from the cell.

The experimental oscillograms are shown in Fig. 6. The upper oscillogram pertains to the case when both pump components, strong and weak, are quasicontinuous; the pulse reflected from the cell in the nonthreshold regime duplicates in shape the incident pulse. The lower oscillogram pertains to the investigated RWF of the quasicontinuous pump component in the field of the strong pulse component. It is seen that in this case the Stokes pulse obtained in nonthreshold reflection is close in shape to the strong-pump pulse  $e_0(\eta)$ . This result confirms the theoretical derivation of Eq. (13).

The results demonstrate the following. The reversal



FIG. 6. Oscillograms of the incident pulses of the weak pump component (first) and of those backscattered with inversion of the weak-component wave front (second): upper trace—the durations of the pulses of both components of the exciting radiation are equal; lower—the strong pump component is rectangular in shape and is of 10 nsec duration.

of the radiation wave front in SMBS in the nonthreshold regime makes it possible to realize this method also for sufficiently short pulses whose direct conversion is made difficult by the substantial increase of the pump threshold intensity in the nonstationary regime and by other nonlinear processes (self-focusing, optical breakdown, and others). Nonthreshold reflection in SMBS in media with short lifetime of the acoustic phonons, e.g.,  $CCl_4$  with  $\tau_p \leq 1$  nsec, makes it possible to obtain RWF of pulses of duration  $\tau_p \approx 0.5$  nsec with a reflection coefficient  $R \geq 10\%$ .

4. The RWF process employed here can be regarded as four-photon interaction of two pump waves ( $e_0\mathcal{E}_0$  and  $e_1\mathcal{E}_1$ ) and two Stokes components ( $c_0\mathcal{E}_0^*$  and  $c_1\mathcal{E}_1^*$ ). As a result of the interference of the waves  $e_1\mathcal{E}_1$  and  $c_0\mathcal{E}_0^*$  there is excited in the medium a hypersonic grating of frequency  $\Omega = \omega_1 - \omega_{s0}$ , from which the  $e_0\mathcal{E}_0$  component is scattered into the  $c_1\mathcal{E}_1^*$  wave, and in the general case the Stokes component  $c_0\mathcal{E}_0^*$  can be transmitted from the outside, while the wave  $e_0\mathcal{E}_0$  can have a frequency  $\omega_0 = \omega_1 + \omega_{s0} - \omega_{s1}$  that differs (within the limits allowed by the wave detuning  $\delta k = k_1 - k_{s0} + k_{s1} - k_0$ ) from the frequency  $\omega_1$  of the wave  $e_1\mathcal{E}_1$ . It must be noted that reflection can be effected both with downward frequency conversion (Stokes component), as first observed in Ref. 1, and upward (anti-Stokes component), which was observed in Ref. 6.

The scheme considered by us has the advantage over the standard scheme using RWF with degenerate four-photon mixing, inasmuch the strong backward Stokes wave is in this case also the result of RWF and is therefore always perfectly tuned, and furthermore at practically any structure of the forward-wave front, not only a plane one. Furthermore, in schemes based on the degenerate four-photon mixing there can arise the instabilities of opposing pump beams which are typical of self-focusing in cubic media.

Nonthreshold reflection with RWF has also selectivity: the signal power is nonthreshold reflection decreases with increasing signal spectral width. As a result, the reflection of broadband noise, say due to luminescence of the amplifying neodymium stages, can be strongly suppressed compared with the signal reflection, and this is of great significance when it comes to obtaining high radiation contrast in high power installations.

In conclusion the authors thank N. G. Basov for stimulating discussions and support, and V. I. Bespalov and I. M. Bel'dyugin for a discussion of individual aspects of the article.

<sup>1</sup>If the power of wave  $c_0 \mathcal{E}_0^*$  is higher than that of wave  $e_0 \mathcal{E}_0$ , as can be done in the case of two cells by placing an amplifier between them, then the reflection of the weak component  $e_1 \mathcal{E}_1$  can be accompanied by amplification.

<sup>1</sup>N. G. Basov, I. G. Zubarev, A. V. Kotova, and M. G. Smirnov, *Kvantovaya Elektronika* (Moscow) **6**, 394 (1979) [*Sov. J. Quantum Electron.* **9**, 237 (1979)].

<sup>2</sup>V. I. Bespalov, A. A. Betin, and G. A. Pasmanik, *Izv. Vyssh. Ucheb. Zaved.* **21**, 961 (1978).

<sup>3</sup>V. G. Sidorovich, *Zh. Tekh. Fiz.* **46**, 2168 (1976) [*Sov. Phys. Tech. Phys.* **21**, 1270 (1976)].

<sup>4</sup>S. A. Akhmanov and A. S. Chirkin, *Statisticheskie yavleniya v nelineinoi optike* (Statistical Phenomena in Nonlinear Optics), *Izd. MGU*, 1971.

<sup>5</sup>I. G. Zubarev and S. I. Mikhailov, *Kvantovaya Elektronika* (Moscow) **1**, 1239 (1974) [*Sov. J. Quantum Electron.* **4**, 683 (1974)].

<sup>6</sup>V. I. Bespalov, A. A. Betin, G. A. Pasmanik, and A. A. Shilov, *Pis'ma Zh. Tekh. Fiz.* **5**, 242 (1979) [*Sov. Tech. Phys. Lett.* **5**, 97 (1979)].

Translated by J. G. Adashko

## Modulation oscillations of a light wave in the Stark-pulse technique

A. I. Alekseev and A. M. Basharov

*Moscow Engineering Physics Institute*

(Submitted 18 January 1979)

*Zh. Eksp. Teor. Fiz.* **77**, 537-547 (August 1979)

A theoretical investigation is made of the modulation oscillations of the intensity of a light wave in a gas medium perturbed by two Stark pulses of a constant electric field. The echo phenomena that occur both during the time of action of the second Stark pulse and after this pulse are investigated. New photon-echo manifestation, in the form of induction echo and nutation echo, are established. The first is formed on the basis of free optical induction, and the second on the basis of optical nutation. A new modification of the edge echo that appears after the action of only one perturbing Stark pulse is also investigated. The new echo phenomena, just as those previously observed, make it possible to determine the dipole moments of atomic transitions, the time of irreversible relaxation in a medium, as well as the Stark level shifts.

PACS numbers: 51.70. + f, 32.60. + i

Brewer and Shoemaker<sup>1,2</sup> have proposed an original procedure for the investigation of optical nutation, of free optical induction, and of photon echo. In this procedure, the gas medium is located for a long time in the field of a monochromatic wave whose frequency  $\omega$  is close to the frequency of some atomic transition. As a result of the Doppler effect the frequencies of this transition in the gas atoms are scattered about the principal value  $\omega_0$ . Inside the Doppler contour there are therefore two groups of atoms, one at resonance with the monochromatic wave, and the other not. All the atoms are subjected for a short time  $\tau$  to the action of a strong constant electric field (a Stark pulse). The Stark effect shifts the energy levels, so that for the resonant atoms the application of the Stark pulse is equivalent to the vanishing of the monochromatic wave. At the same time the nonresonant atom become resonant with the monochromatic wave after the application of the Stark pulse and react thus as if they were exposed to a light pulse of frequency  $\omega$  and duration  $\tau_1$ . The reradiation of the photons produces modulation oscillations of the monochromatic-wave intensity, and a second application of a Stark pulse of duration  $\tau_2$  is accompanied by a photon echo. This Stark-pulse technique was subsequently employed in many experiments (see, e.g., Refs. 3-7).

The optical nutation and the free induction produced by a single Stark pulse were considered by Hopf, Shea, and Scully.<sup>8</sup> Yet no theoretical investigation has been

made so far of the modulation oscillations of the light wave under the influence of two successive Stark pulses. For a qualitative explanation of photon echo, use was made<sup>1,3,5,7</sup> of the physical concepts previously employed in the problem of the passage of two short light pulses through a gas.<sup>9,10</sup> This explanation, however, must be substantiated.

We present below a unified description of optical nutation, free optical induction, and photon and edge echo, which are observed in the Stark-pulse technique. In addition to the traditional pulse echo produced after the second Stark pulse, we describe new nonlinear effects that evolve within the time interval that the second Stark pulse is on and after the pulse. The approach proposed has made it possible to establish that only in the experiment of Glorieux *et al.*<sup>5</sup> does the formation of the photon echo under certain conditions proceed in the same manner as when the medium is excited by two light pulses.<sup>9,10</sup> In both cases (Ref. 5 and Refs. 9 and 10) is the echo formed on the basis of free optical induction. Yet in other experiments<sup>1,3,7</sup> the produced echo is of different origin and is differently described, since it is formed on the basis of optical nutation.

### 1. CALCULATION METHOD AND BASIC FORMULAS

Assume that a light wave

$$\mathbf{E} = \mathbf{E}_0 e^{i(\omega t - \mathbf{k} \cdot \mathbf{r})} + c.c. \quad (1)$$